32nd Electric Vehicle Symposium (EVS32)
Lyon, France, May 19 - 22, 2019

Iron Loss Modelling of Electrical Traction Motors for Improved Prediction of Higher Harmonic Losses

Jan Rens[1], Lode Vandenbossche[2], Ophélie Dorez[3]

[1]*ArcelorMittal Global R&D Gent, OCAS, Pres. J. F. Kennedylaan 3, B-9060 Zelzate, Belgium*

[2]*(corresp. author) ArcelorMittal Global R&D, Technologiepark 48, B-9052 Zwijnaarde (Gent), Belgium, lode.vandenbossche@arcelormittal.com*

[3]*ArcelorMittal Saint-Chély d'Apcher, Rue des Martyrs du Maquis, F-48200 Saint-Chély d'Apcher, France*

Summary

A Finite Element (FE) modelling approach is presented to account for the core losses in electrical machines that are generated by higher harmonic frequencies, for example caused by Pulse Width Modulation (PWM) switching or by space harmonics due to the machine geometry. The model builds further on a post-processing calculation tool that was recently developed to take into account the magnetic skin effect in electrical steel laminations at high frequencies, but extends this by a more detailed loss analysis of the minor hysteresis loops that are caused by the higher harmonics. Further, these tools for high-frequency loss analysis are integrated into a complete electrical machine model with separate consideration of the major and minor loops. The modelling approach relies strongly on extensive magnetic measurement data of the electrical steel in order to accurately predict the different loss components for minor hysteresis loops, as a function of the DC bias field, frequency and amplitude of the minor loop. Results from the model are shown for an automotive traction motor, illustrating the losses caused by PWM harmonics and demonstrating the relevance of including the skin effect in these calculations.

Keywords: finite element calculation, motor design, efficiency, harmonics

1 Introduction

ArcelorMittal has developed iCARe®, a specific product line of electrical steels which are optimised for automotive traction electrical machines. In order to further reduce the magnetic core losses of these electrical steels for wide frequency operation, research is ongoing into the modelling of various mechanisms of core loss dissipation. The main obstacle to the accurate prediction of the efficiency of traction motors for electric transport vehicles remains the calculation of the core losses, as they can be strongly affected by a number of factors that are not yet fully understood. In general, the magnetic core losses that are measured on an electrical machine are significantly higher compared to those measured on an electrical steel sheet, which may be due to material degradation from cutting techniques, operation at high temperature and the presence of mechanical stresses introduced during assembly. Also, the presence of higher harmonics in the magnetic polarisation waveforms, due to a high magnetic utilisation of the material and to inverter-fed operation, will result in additional losses, minor loops and a potentially strong skin effect in the laminations.

A general and widespread approach to core loss modelling is based on the separation of losses into hysteresis, excess and eddy current loss components, according to the statistical loss theory of Bertotti [1]. When such an approach is implemented in the frequency domain, the losses that are generated by each harmonic of the magnetic polarisation waveforms are analysed separately and summed to obtain the overall loss figure. If the model parameters are tuned appropriately based on sufficient experimental data that reflects the wide operating range of traction motors, it becomes possible to predict the effects of material degradation due to cutting, elevated temperature and mechanical stresses by including the relevant experimental data [2]. However, when it comes to the prediction of losses that are caused by higher harmonics of the magnetic polarisation, the aforementioned model is reaching its limitations, as it does not take into account any skin-effects, and moreover this model is generally based on an extrapolation of magnetic measurements at low frequencies and at zero bias fields. Although skin-effect calculations have previously been presented [3], the skin effect was not yet integrated into a more general loss model for electric machines. It is the scope of this paper to develop a modelling approach which is still based on the statistical loss theory and the separation of losses, but which explicitly includes the calculation of skin effect and minor loop losses to account for losses caused by high harmonic frequencies. For this, it becomes interesting to revert to a time-domain model instead of a frequency-domain model.

In order to calculate the skin effect within a lamination, the most precise calculation would require the development of finely-meshed three-dimensional (3D) FE models, which must be solved transiently because of the non-linearity of the magnetization curves. Because the solution of these models involves a high computational cost, a number of simplified calculation methodologies have been proposed in literature based on two-dimensional (2D) FE analysis. For example, analytical equations can be used as a post-processing tool to describe the flux distribution in a lamination in case a linear material model can be adopted [5]. More advanced methods extend the 2D model with a one-dimensional (1D) FE modelling approach. In this case, the 1D model is solved in the direction of the thickness of the lamination, in combination with the 2D model in the plane of the lamination where homogeneous material properties are assumed [4]. As a result of the coupled 2D-1D calculation approach, it also becomes possible to include the reaction fields from the eddy currents into the field calculations, as well as to predict the eddy current losses in the lamination, taking into account saturation effects.

This paper will introduce an iron loss model which is implemented in the time-domain and which explicitly includes the assessment of skin effect and minor loops. First, both conventional modelling approaches based on the frequency-domain and time-domain will be discussed. Then, a calculation methodology to account for skin effect is presented and validated with measurements. Finally, iron loss simulations on a permanent magnet traction motor for electric vehicles will be discussed and compared with conventional modelling techniques.

2 Theoretical analysis of loss models which do not account for skin effect

As discussed previously, all models discussed in this work are based on the statistical loss theory, which relies on the physically-based concept of separation of losses into hysteresis, excess and classical eddy current components:

$$P = P_{hyst} + P_{exc} + P_{class} \tag{1}$$

For fixed frequencies, the above equations can be re-written in terms of the energy-loss per cycle $W = P/f$

$$W = W_{hyst} + W_{exc} + W_{class} \tag{2}$$

In these equations, the hysteresis loss is often referred to as the quasi-static loss, and its energy-loss per cycle can be assumed to be independent of frequency. The excess and classical loss together are often called the dynamic losses, as they are generated by induced electrical currents that are caused by time-varying magnetic fields in the material. For the dynamic losses, the energy loss per cycle strongly depends on frequency. In the classical theory, where the magnetic domain structure is ignored, the induced currents are distributed homogeneously throughout the thickness of the sheet, resulting in the derivation of the classical loss

component. The excess loss component was introduced to account for the magnetic domain structure, which results in currents that are not homogeneously distributed but centred around moving domain walls.

Although the loss components are frequently calculated from the polarisation waveforms in the frequency domain, this study is focussed on equations in the time-domain. Equivalent formulations for the frequency domain can be found elsewhere [2]. Time-domain modelling requires the formulation of the instantaneous power loss *p(t)* for periodic waveforms of the polarisation, which is then integrated over time to obtain the average losses.

Quasi-static loss component:

As hysteresis loss does not depend on the dynamics of the waveform, the hysteresis loss of an arbitrary waveform with peak amplitude J_p can be written as.

$$P_{hyst} = W_{hyst}(J_p) f_0 = s_{hyst} J_p^{(\alpha+\beta J_p)} f_0 \tag{3}$$

where s_{hyst}, α and β are fitting parameters for the studied electrical steel grade, based on measured Epstein data and f_0 is the fundamental frequency of the periodic waveform. Because W_{hyst} does not depend on the dynamics of the waveform, it can be directly measured via quasi-static magnetic measurements. Hysteresis losses can thus only be established a posteriori when the BH loop is closed. In order to include the effect of rotational magnetisation as compared to alternating magnetisation for which the formulas are generally derived, an adaptation of the above equation can be formulated:

$$P_{hyst}(J_p, f) = s_{hyst}\left(1 + \left(r(J_p) - 1\right)c\right) J_p^{(\alpha+\beta J_p)} f_0 \tag{4}$$

where $r(J_p)$ is a rotational loss factor (empirical loss function, experimentally determined on a few grades) and c is the local flux-distortion factor, defined as $c=J_{min}/J_p$.

Excess dynamic loss component:

In the statistical loss theory, excess losses are analysed by considering the magnetisation process as the result of n simultaneously active magnetic objects that are randomly distributed in the sample cross-section. A simplified formulation for instantaneous excess loss power dissipation can be given by [5]:

$$p_{exc}(t) = \sqrt{\sigma G S V_0}\left(\frac{dJ(t)}{dt}\right)^{1.5} \tag{5}$$

where σ is the electrical conductivity, $G = 0.1356$ is a dimensionless constant, S is the cross-sectional area of the lamination and V_0 is a parameter that depends on J_p and defines the statistics of the n magnetic objects.

Classical dynamic loss component:

Under the assumption of a homogeneous distribution of the current density, the instantaneous classical loss $p_{class}(t)$ due to eddy currents is given by:

$$p_{class}(t) = \frac{\sigma d^2}{12}\left(\frac{dB}{dt}\right)^2 \approx \frac{\sigma d^2}{12}\left(\frac{dJ}{dt}\right)^2 \tag{6}$$

where d is the thickness of the lamination sheet and B the flux density, which is identical to the polarisation J in practical terms.

Overall core loss model:

The total average core loss resulting from an arbitrary periodic polarization waveform with period T_p is obtained from the combination of the previously discussed loss components:

$$\begin{aligned} \mathrm{P} &= P_{hyst} + P_{exc} + P_{eddy} \\ &= s_{hyst}\left(1 + \left(r\left(J_p\right) - 1\right)c\right) J_p^{\left(\alpha+\beta J_p\right)} f_0 + \frac{1}{T_p}\int_0^{T_p} p_{exc}(t)dt + \frac{1}{T_p}\int_0^{T_p} p_{class}(t)dt \end{aligned} \tag{7}$$

3 Modelling of skin effect

At high electrical frequencies, the above formulations will become increasingly inaccurate due to the onset of the skin effect, which results in a redistribution of the flux within the lamination and thus affects all loss components. This effect is shown in Fig. 1a , which shows an FE calculation of the flux density distribution in half of a 0.3mm lamination when a 10kHz magnetic polarisation waveform with a peak value of 0.15T is applied through the lamination. The corresponding current density distribution is shown in Fig. 1b. For linear materials and sinusoidal waveforms, the skin depth or penetration depth δ of the magnetic flux into the lamination can be conveniently calculated as:

$$\delta = \frac{1}{\sqrt{\pi \mu f \sigma}} \tag{8}$$

where μ is the permeability of the material. It could be shown that for a 0.3mm thick 3%Si electrical steel which has a high peak value of permeability, the skin depth would already reach values smaller than half the thickness of the lamination at frequencies below 1kHz, when a linear behaviour would be assumed. For small variations of the magnetic polarization around a given bias offset, a non-linear material will behave linearly, with a permeability equal to the incremental relative permeability at the bias polarization. Therefore, the above equation can be used to estimate the skin depth in non-linear materials, provided the magnitude of the flux density remains small, as is often the case with higher harmonic disturbances.

In order to accurately calculate the distribution of magnetic flux and current within the lamination, it is necessary to compute Maxwell's diffusion equation. For electrical steel laminations, the representation is often simplified to a one-dimensional problem in the direction of the lamination, with only half the lamination modelled, as schematically shown in Fig. 1c. This leads to a simplified one-dimensional diffusion equation in the z-direction:

$$\frac{\partial^2 H(z,t)}{\partial z^2} = \sigma \frac{\partial B(z,t)}{\partial t} \tag{9}$$

for which a number of calculation methodologies exist. The use of the 1D approach is valid as long as the lateral dimensions of the lamination are large in comparison to its thickness, because the return paths of the current, i.e. the end effects, are ignored.

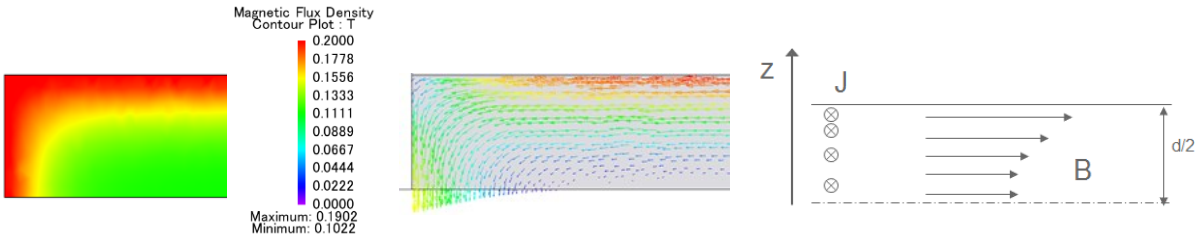

Figure 1 a) Flux density profile in half a lamination of 0.3mm when an average sinusoidal flux density is applied with an amplitude of 0.15T at 10kHz
b) corresponding current density distribution in lamination
c) 1D model for the calculation of skin effect, where all parameters only depend on the z-dimension.

3.1 Analytical modelling of eddy current loss

When the material exhibits a linear permeability and for sinusoidal excitation, an analytical solution can be found for eq. 9 [4]:

$$H(z) = j\omega\sigma B_p \frac{d}{2} \frac{cosh(kz)}{k \sinh(kd/2)}, \text{ with } k = \frac{1+j}{\sqrt{2}}\sqrt{\omega\sigma\mu} \tag{10}$$

with σ the electrical conductivity, ω the electrical pulsation and B_p the peak value of the average flux density through the material. The resulting eddy current loss density can then be calculated as follows:

$$W_{class}(J_p, f) = \frac{\pi}{2}\frac{\lambda J_p^2}{\mu}\frac{\sinh\lambda - \sin\lambda}{\cosh\lambda - \cos\lambda}, \text{ with } \lambda = \sqrt{\pi\sigma\mu d^2 f} \tag{11}$$

3.2 Non-linear post-processing calculation using a Finite Difference modelling

A non-linear calculation methodology of the 1D problem has been derived in [6], by dividing the lamination in a numbers of layers with constant flux and current densities, as given in equations 12:

$$\frac{dB_1}{dt} = \frac{8H_2 - 7H_1 - H_3}{2\sigma h^2} + \frac{3(N-1)}{w_1 S}u(t) \tag{12}$$

$$\frac{dB_i}{dt} = \frac{H_{i-1} - 2H_i + H_{i+1}}{\sigma h^2}, \quad (i = 2, \dots, N-1)$$

$$\frac{dB_N}{dt} = \frac{2(H_{N-1} - H_N)}{\sigma h^2}$$

where B_1, B_2, .., B_N the flux densities in each of the N layers
H_1, H_2, …,H_N the magnetic fields in each layer
h the thickness of each layer
$u(t)$ the applied voltage over the winding with turns w_1
S the cross-sectional area of the core

Within each layer the normal non-linear constitutive relationships are valid. As this methodology requires the solution of transient differential equations, dynamic solvers are required which are available in for example Python or Matlab/Simulink.

As an example of the result from this methodology, Fig. 2a shows the magnetic polarization waveforms in the inner and outer layers of an electrical steel with 0.3mm thickness, when an average sinusoidal flux-density of 0.5T at 2kHz is applied. Here, a clear skin effect can be noticed, with a larger polarization near the outer edge, a phase shift between polarization waveforms throughout the thickness, and the strong non-linear behavior even though the total flux through the lamination is forced to be sinusoidal. Fig. 2b shows similar waveforms when the average polarisation is 1.5T at 2kHz. In this case however, the material starts to saturate near the edge of the lamination, such that the peak polarisations near the skin cannot rise above the average value, resulting in an identical peak value throughout the lamination. However, non-linearity and phase differences between the waveforms are apparent.

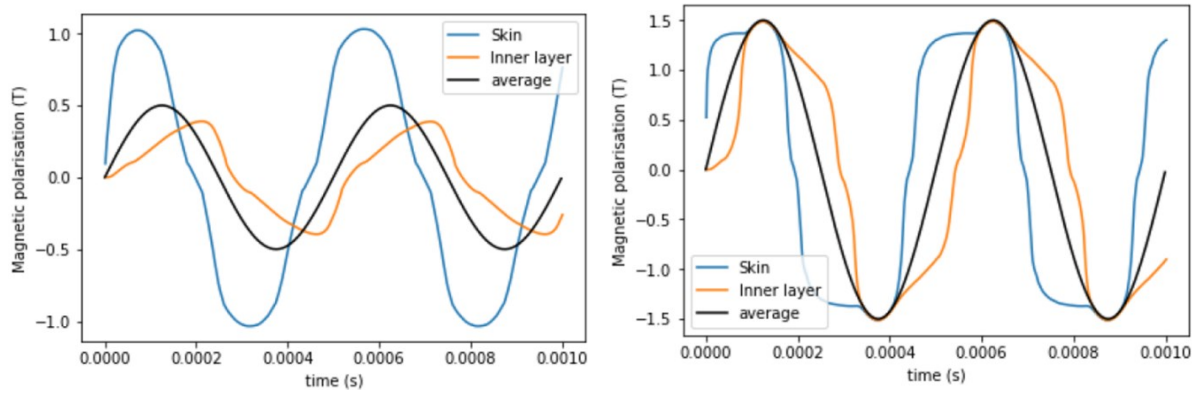

(a) (b)

Figure 2 Flux density distribution within a lamination, when the average flux density is enforced to be a sinewave with a) average B_{pk} = 0.5T at a frequency of 2kHz and b) average B_{pk} = 1.5T at a frequency of 2kHz

Having calculated the flux-density distribution, it becomes possible to predict the current density distribution and the resulting eddy-current losses. Fig. 3 compares the loss constant for the previously defined calculation methodologies, i.e. the classical Bertotti calculation, the linear analytical formulation and the non-linear formulations, for two different averaged flux-density waveforms that are applied to the material. It can be seen that for low frequencies, in the absence of skin-effect, the three methods give identical results. At high frequencies, however, the analytical and non-linear calculations both predict lower losses compared to the situation when no skin-effect would be present. In other words, due to the skin effect, the current density in

the material will not increase linearly any more with frequency, resulting in a slower increase in losses with frequency than would be expected without skin effect.

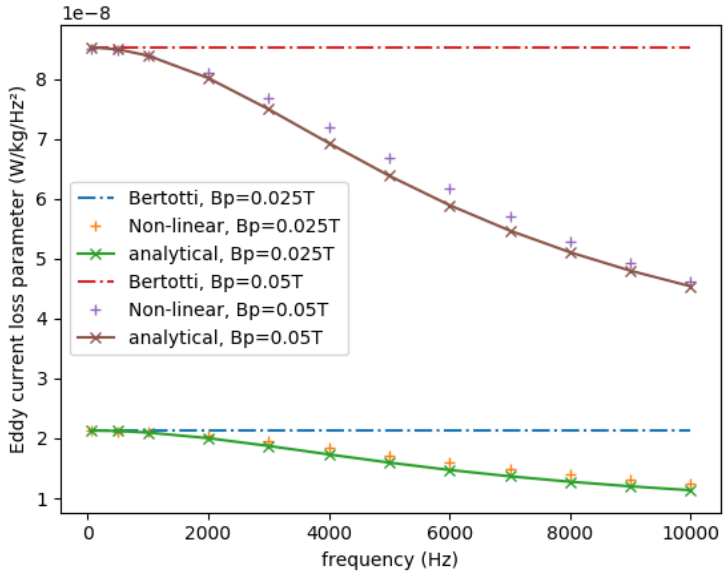

Figure 3 Comparison of eddy-current loss constant, calculated using three different methodologies, for 2 average sinusoidal waveforms of small amplitude.

As the previous figure showed a good agreement between the linear and non-linear analysis for waveforms with small amplitude, Fig 4a and b, compares magnetic polarization waveforms in the skin and near the centre of the material for high-frequency polarization waveforms with small amplitude. Further, a DC bias polarization was added to the waveforms in the figure, in order to make the waveforms more representable for higher harmonics that are due to for example switching frequencies. As can be seen, for these small amplitudes, both linear and non-linear models predict similar polarization waveforms, suggesting that a non-linear analysis may not be required and that the analytical calculation methodology could be sufficient. It can also be noted from the figures that a transient effect is present in the solution of eq. 12, such that a few periods must be simulated to obtain a stable steady-state solution.

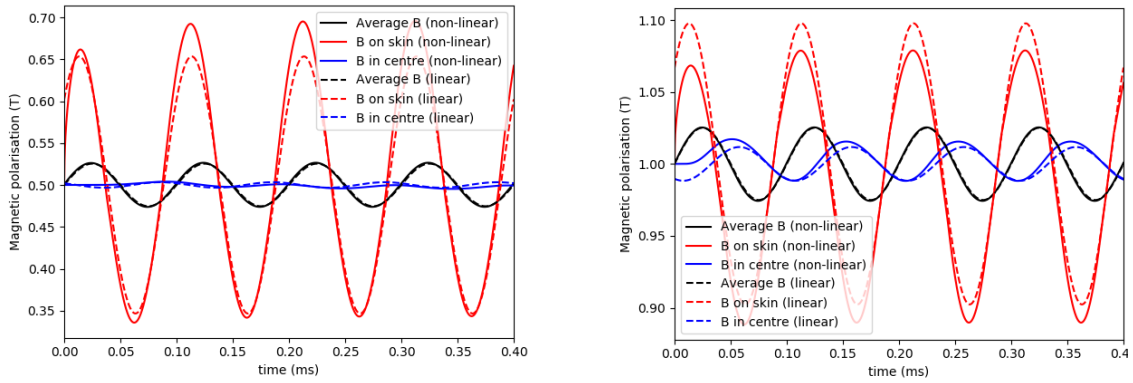

(a) (b)

Figure 4 a) polarisation waveforms in the material (near centre, near skin and average) for an average waveform of 0.025T at 10kHz, superposed on a DC bias polarization of 0.5T
b) polarisation waveforms in the material (near centre, near skin and average) for an average waveform of 0.025T at 10kHz, superposed on a DC bias polarization of 1T

3.3 FE modelling of eddy current loss

Finally, commercial FE packages can also be used to account for the skin effect. Certain softwares have implemented the approach where conventional 2D models with homogeneous material properties are operated in combination with a 1D model at each node of the model. This coupled 2D-1D modelling approach thus allows to calculate eddy current losses for an arbitrary transient excitation, taking into account non-linearities and also allowing a coupling between eddy current losses with the field calculation itself. However, the models are generally available as a black-box tool predicting eddy-current loss only, and it is not possible to assess the actual flux density distribution in the depth of the lamination. Further, the computation may suffer from long computation times and convergence problems. Naturally, apart from the 2D-1D analysis mentioned above, accurate predictions can be obtained through brute-force 3D modelling of the lamination, however at a large computational cost.

3.4 Skin effect regarding hysteresis and excess loss

Because the skin effect results in a redistribution of the polarisation across the thickness of the lamination, the density of the hysteresis loss is no longer homogeneous within the lamination. Therefore, the quasi-static energy loss per cycle can be calculated as the average loss density across the thickness [4]:

$$W_{hyst}(J_p, f) = \frac{1}{d}\int_{-d/2}^{d/2} s_{hyst} J_p(z)^{(\alpha+\beta J_p(z))} dz \tag{13}$$

with s_{hyst}, α and β given in eq. 3 and determined from measurements at sufficiently low frequencies where skin effect does not come into play. It can be understood that the skin effect will result in an increased hysteresis loss, because the loss density is expected to increase with increasing polarization ($\alpha+\beta J_p > 1$). However, the effect on the total losses may be small as dynamic losses are dominant at such high frequencies.

In fact, it is expected that the major hysteresis loop will not cause considerable skin effects and that losses can still be calculated in the conventional way, unless the fundamental frequency would be sufficiently high. Minor loops, however, would always require some assessment of the skin effect. Further, as will be shown later, the parameters that describe hysteresis are sufficiently different for minor and major loops, such that a separate treatment of major and minor loops is necessary.

In this study, excess losses are assumed to be independent of the skin effect and only affected by the peak polarisation of the loop [4]. Further, it is assumed that the coefficient V_0 that is used to calculate the excess loss (eq. 5) depends on the incremental permeability at the point where minor loop and major loops are connected. For small amplitudes of the minor loop, the following equation can then be used [4]:

$$V_0(J_m, J_b) \approx V_0(J_m, J_b = 0)\frac{|\mu(J_m, J_b=0)|}{|\mu(J_m, J_b)|} \tag{14}$$

where J_m and J_b are the peak amplitude and bias polarization of the minor loop, respectively.

4 Overall modelling approach

The overall methodology for the calculation of global core losses in an electrical machine is schematically shown in Fig. 5. The approach is based on a finite-element model of the electrical machine, where the waveforms are simulated over a single electrical period with a large number of timesteps. In a post-processing procedure, the resulting waveforms of the magnetic field and polarisation are then analysed for each mesh element, allowing for the prediction of the various core loss components within each element. The methodology further relies heavily on measured material data, both for establishing the anhysteretic magnetisation curve that is input to the FE model, as well as for identifying material-specific core loss parameters at the operating conditions that are simulated in the model. The underlying methodology in the post-processing calculations is based on the time-domain formulations given previously in section 2. It can readily be understood that the approach also allows to account for the effects of material degradation due to manufacturing techniques, mechanical stresses or elevated temperatures, as has been reported previously for frequency-domain core loss models [2].

For this study, the polarisation waveforms that are obtained for each element were subdivided into the major and minor loops, which were treated differently. Where the major loop is analysed according to the standard approach, the calculations for the minor loops include the skin effect and are based on specific parameters for the calculation of quasi-static hysteresis loss.

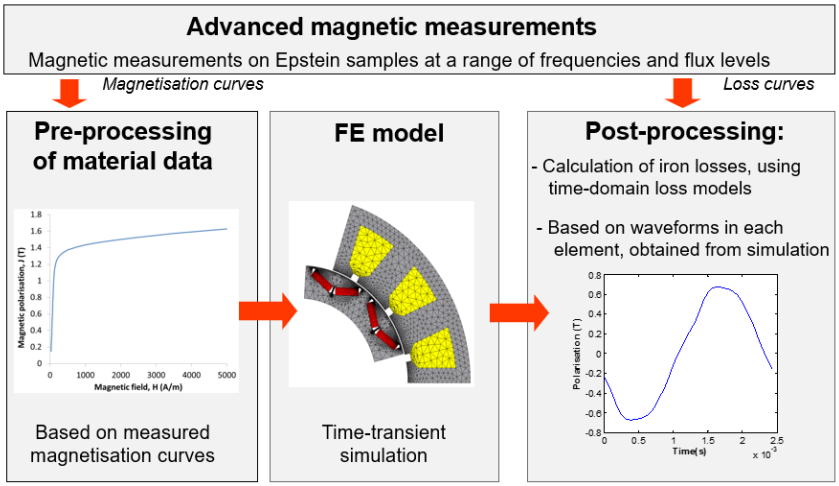

Figure 5 General overview of the numerical scheme of the ArcelorMittal iron loss modelling approach

5 Experimental verification of skin effect model

A number of laboratory tests were carried out on a 0.3mm thick 3%Si electrical steel for automotive applications, in order to verify the skin effect formulations discussed in section 3, and to give a validation of the overall modelling approach as explained in section 4. Also, quasi-static magnetic measurements were conducted for small-amplitude waveforms superimposed on a DC bias polarisation, in order to derive hysteresis fitting parameters for the minor loop analysis. Finally, a 50Hz waveform with superposed harmonics was measured and compared with simulation results.

5.1 Sinusoidal waveforms without DC offset

Conventional magnetic measurements were conducted up to a frequency of 20kHz with polarisation levels up to 0.15T. From the total losses that were measured, the eddy current component was estimated as follows:

$$P_{eddy} = P_{measured} - P_{hyst\_skin} - P_{exc} \tag{15}$$

where P_{hyst_skin} refers to the hysteresis losses that have been corrected for the skin effect, and where P_{exc} refers to the excess loss based on the average flux density in the lamination. Fig. 6 shows a comparison between the eddy current loss constant, k_{eddy}, that was obtained from measurement and various calculation methodologies, where k_{eddy} was defined as the volumetric loss divided by the square of the frequency. It can be seen that both analytical and FE methods are able to predict the downward slope of the measured curve, whereas the classical analysis from Bertotti which ignores the skin-effect overestimates the eddy current losses at elevated frequencies.

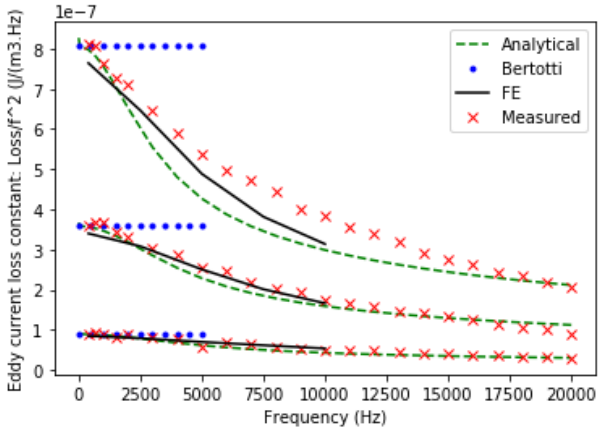

Figure 6 Measured and predicted eddy current loss density per frequency, for sinusoidal polarizations with peak flux density of 0.05T, 0.1T and 0.15T

5.2 Quasi-static measurements at DC bias

In order to investigate the hysteresis loss that is dissipated in minor loops, measurements were conducted where quasi-static minor loops were generated for a range of amplitudes and DC bias levels. Because the measurement system is not capable to measure a DC bias field, a slow-varying waveform was actually used, with the minor loop occurring at the peaks of this loop, as shown in Fig. 7a. Fig. 7b shows the resulting minor loops for an amplitude of 0.05T with different bias values. As can be seen from the area of the respective loops, the hysteresis loss of a minor loop increases significantly with increasing DC bias field. Therefore, a mapping was obtained through measurement of a range of amplitudes and DC offsets, to allow the prediction of hysteresis loss of minor loops as a function of amplitude and bias field for later analysis.

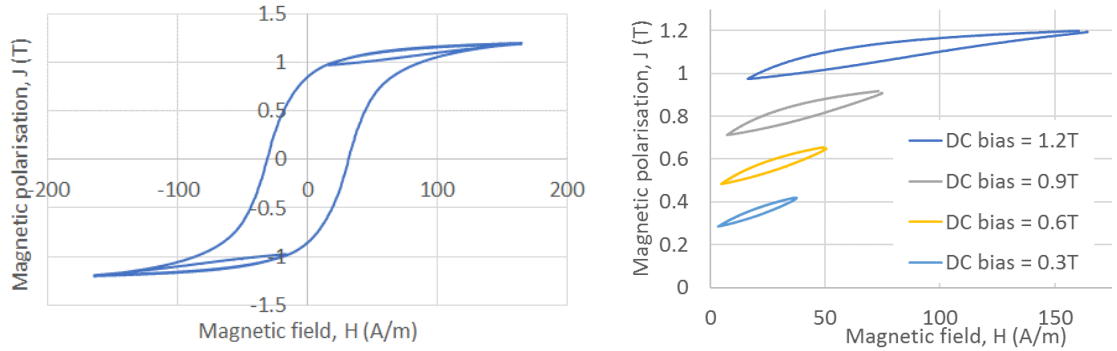

(a) (b)

Figure 7 a) Quasi-static waveform which includes a quasi-static minor loop
b) shape of quasi-static minor loops for different DC bias fields

5.3 Verification on a waveform with high-frequency harmonics

In order to assess the overall modelling approach, an Epstein frame was used to measure core losses when the material is subject to a 50Hz, 0.9T waveform that was generated via a PWM scheme with a switching frequency of 4kHz. The measured BH-loop is shown in Fig. 8a, whereas the measured polarisation waveform is shown in Fig. 8b. On this figure, the fluctuations that result in minor loops and for which separate calculations are run are indicated in red. The result of this analysis are summarised in Table 1 for different calculation methods. Here it can be seen that for this example, all calculations provide a satisfactory answer. However, since the frequency-domain model predicts almost all of its power loss to be at the fundamental frequency, it does not properly separate losses. The model which includes a separate calculation for minor loops is the only one that can correctly separate losses, as it was measured that the presence of the harmonics added around 15% of losses.

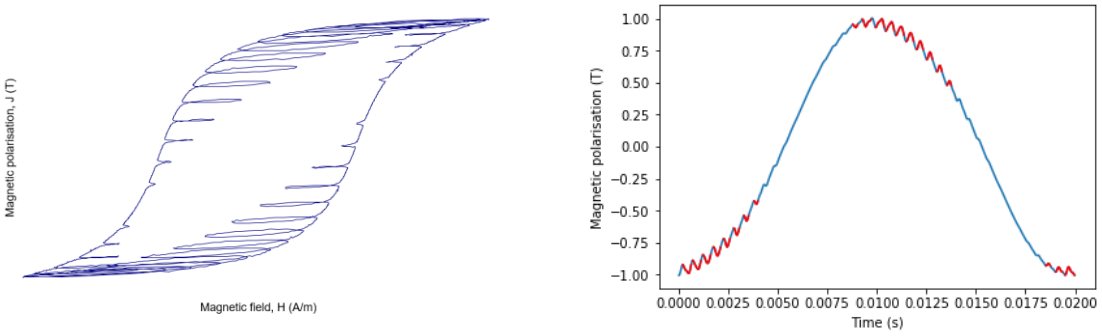

(a) (b)

Figure 8 a) Measured BH-waveform for a 50Hz, 0.9T sinusoidal polarisation that was generated via a PWM scheme b) corresponding measured polarisation waveform. The minor loops that are separately calculated are marked in red.

Table 1: comparison of loss predictors for the data shown in Fig. 8, for which a total loss of 0.967W/kg was measured

Methodology	*Total loss*
Frequency-domain	1W/kg from which 0.97W/kg at the first harmonic
Time-domain without skin effect	0.97W/kg
Time-domain with skin effect and minor loops	0.95W/kg from which 0.15W/kg at all minor loops

6 Application to modelling of traction motor

The electrical machine model shown in Fig. 9 is used as a reference for further analysis of the modelling approach. The machine is a 10 pole, 15 slot, interior permanent magnet (IPM) machine, which was designed for an automotive traction application, with specifications shown in Table 2. A fractional slot stator topology with concentrated windings was chosen in order to achieve a high torque density, however resulting in considerable space-harmonics. The core is made from an electrical steel from the ArcelorMittals iCARe® range, which was especially designed to reach high efficiencies up to elevated frequencies. As shown in Fig. 9, only 1 pole-pair of the machine is modelled due to symmetry. For this machine, a previous study had already shown that the calculation of the skin effect did not significantly change the total core loss behaviour, when the motor is supplied by sinusoidal waveforms. For this analysis, the motor was simulated at 4800rpm and supplied with a three-phase PWM waveform with carrier frequency of 16kHz, by using the standard library function that is implemented in the JMAG software. A timestep of 4.1µs was used for the simulation. As discussed previously, the resulting waveforms in each element were analysed, with a separate assessment of major and minor loops.

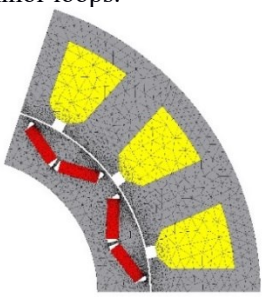

Figure 9 FE mesh of IMP SM machine

Table 2: Principal motor specifications

Outer diameter	195mm
Axial length	171mm
Nominal power	50kW
Maximum torque	150Nm
Maximum speed	12000rpm

Table 3 compares the calculated losses, when respectively a frequency-based model, a standard time-based model, and a time-based model where minor loops and skin effect are taken into account.

Table 3: Motor core loses calculated using different methodologies

Frequency-domain	546W
Time-domain without skin effect	665W
Time domain with skin effect and minor loops	678W

It can be noted that the frequency-domain model predicts considerably smaller loss generation compared to the time-based models. The model where minor loops are accounted for allows for the assessment of the losses that are generated by the higher harmonics. This appeared to be around 15% of the total core losses.

7 Conclusions

A framework has been described to predict iron losses of electrical machines, including skin effect and the presence of minor loops. For the analysis of the model, an electrical steel was selected from ArcelorMittal's iCARe® range, which is a product portfolio of electrical steels with enhanced properties that has specifically been developed to meet the high requirements of automotive traction motors. Laboratory magnetic measurements at high frequencies showed good agreement with the theoretical behaviour of the material at high frequencies. Further, numerical calculations on an IPM motor were carried out to assess the importance of skin effect on the predicted losses. It was concluded that accounting for skin effect leads to somewhat higher predicted losses, although the effect remains limited. From this modelling approach, it appears that the PWM supply adds around 15% additional loss to the core of the machine.

References

[1] G. Bertotti, *"Physical interpretation of eddy current losses in ferromagnetic materials",* J. Appl. Phys., vol. 57, 1985

[2] L. Vandenbossche, S. Luthardt, S. Jacobs, S. Schmitz, E. Attrazic, *"Iron Loss Modelling of a PMSM Traction Motor, Including Magnetic Degradation due to Lamination Laser Cutting",* EVS30 Symposium, 2017

[3] J. Rens, S. Jacobs, L. Vandenbossche, E. Attrazic, "*Improved Core Loss Modelling of Electrical Traction Motors through simulation of Skin-Effect in Laminations"*, EVS31 Symposium, 2018

[4] H. Zhao, C. Ragusa, O. de la Barrière, M. Khan, C. Appino, F. Fiorillo, *"Magnetic loss versus frequency in non-oriented steel sheets and its prediction: minor loops, PWM, and the limits of the analytical approach",* IEEE Transactions on Magnetics, Vol. 53, No. 11, 2017

[5] E. Barbisio, F. Fiorillo and C. Ragusa, *"Predicting loss in magnetic steels under arbitrary induction waveform and with minor hysteresis loops",* IEEE Transactions on Magnatics, vol. 40, No. 4, 2004

[6] C. Beatrice, S. Dobák, E. Ferrara, F. Fiorillo, C. Ragusa, J. Füzer and P. Kollár, *"Broadband magnetic loss of nanocrystalline ribbons and powder cores",* Journal of Magnetism and Magnetic Materials, vol. 420, 2016

[7] M. J. Hofman and H. Herzog, *"Modeling magnetic power losses in electrical steel sheets in respect of arbitrary alternating induction waveforms: theoretical considerations and model synthesis",* IEEE transactions on magnetics, vol. 51, no. 2, 2015

[8] L. Chang, T. Jahns, R. Blissenbach, "*Characterization and Modelling of Soft Magnetic Materials for Improved Estimation of PWM-Induced iron Loss"*, IEEE Energy Conversion Congress and Expo 2018, pp; 5371-5378

[9] S. E. Zirka, Y. Moroz, P. Marketos, A. J. Moses: "*Viscosity-based magnetodynamic model of soft magnetic materials"*, IEEE transactions on magnetics, 2006

[10] A. Boglietti, A. Cavagnino: "*Iron loss prediction with PWM supply: An overview of proposed methods from an engineering application point of view",* Electric Power Systems Research 80 (2010), 1121-1127

[11] P. Rasilo, W. Martinez, K. Fujisaki, J. Kyyrä, A. Ruderman: "*Simulink model for PWM-Supplied Laminated Magnetic Cores Including Hysteresis, Eddy-current, and Excess Loss"*, IEEE Transactions on Power Electronics, Vol. 34, No. 2, 2019

Authors

Dr ir Jan Rens graduated in electromechanical engineering at the University of Leuven. He obtained his PhD in electrical engineering at The University of Sheffield for his research into the design of reciprocating actuators. Later, he held a position as an electrical motor design engineer at Magnomatics Limited. Currently, he works at ArcelorMittal Global R&D Ghent, where he is conducting research on electromagnetic applications of electrical steels.

Dr. ir. Lode Vandenbossche graduated in electromechanical engineering at Ghent University, where he studied the link between magnetic properties and the microstructure of steels, resulting in a PhD degree for his research about magnetic non-destructive evaluation of material degradation. He then joined ArcelorMittal Global R&D Gent, where he performed research on electromagnetic applications and electrical steel solutions. Currently he is product development engineer for electrical steels at ArcelorMittal Global R&D.

Ophélie Dorez works at ArcelorMittal Saint-Chély d'Apcher, ArcelorMittal's steel plant specialised in non-oriented fully processed electrical steels, where she is responsible for the organisation and follow-up of all production steps during industrial trails aiming for the product development of new electrical steel grades.